

# A parallel matrix-free finite element solver for phase separation in electrode particles of lithium ion batteries

Giuseppe Fabian Castelli<sup>1,\*</sup> and Willy Dörfler<sup>2</sup>

<sup>1</sup> Karlsruhe Institute of Technology (KIT), Institute of Thermal Process Engineering (TVT), Kaiserstr. 12, 76131 Karlsruhe, Germany

<sup>2</sup> Karlsruhe Institute of Technology (KIT), Institute of Applied and Numerical Mathematics (IANM), Englerstr. 2, 76131 Karlsruhe, Germany

We consider a Cahn–Hilliard-type phase field model for phase separation in electrode particles of lithium ion batteries. For the numerical solution we employ a finite element solver together with a variable-step, variable-order time integration method. To overcome the large computational requirements we use a parallel matrix-free approach with a specialized preconditioner. Numerical experiments demonstrate the capabilities of our solver. In particular, we show the dependence of the phase morphology on the applied insertion rate in a two-dimensional circular particle example.

© 2021 The Authors. *Proceedings in Applied Mathematics & Mechanics* published by Wiley-VCH GmbH.

## 1 Introduction

Nowadays lithium ion batteries (LIBs) are well-established energy storage systems with a wide field of applications. However, the performance of LIBs is strongly influenced by coupled chemical and mechanical processes in single electrode particles [1]. For example, special electrode materials, like lithium iron phosphate  $\text{LiFePO}_4$  (LFP), are known to undergo a phase separation during (dis-)charge [2]. When coupling this effect to mechanics, critical stresses may be generated due to large concentration gradients, which eventually may cause particle fracture [1–3].

In the brevity of this article, we neglect the mechanical coupling and focus on the Cahn–Hilliard-type phase field model for phase separation. Due to the high computational effort in solving the model equations, previous studies in literature were limited to either spherical symmetric solutions for spherical particles, e. g., [4], or adapted material parameters, e. g., [5], [2]. Thus, for the simulation of phase separation in arbitrary particle geometries and particularly in crucial parameter regimes we see a high demand for efficient numerical methods.

## 2 Phase Field Modeling of Phase Separation

Following [2, 3] and the references cited therein, we formulate the dimensionless model: Let  $\Omega \subset \mathbb{R}^d$ ,  $d \in \{1, 2, 3\}$ , be a bounded domain representing an electrode particle and let  $T > 0$  be a final simulation time. We define the free energy density  $\psi: [0, 1] \times \mathbb{R}^d \rightarrow \mathbb{R}$  composed of a homogeneous chemical part  $\psi_{\text{ch}}: [0, 1] \rightarrow \mathbb{R}$  and an interfacial part  $\psi_{\text{int}}: \mathbb{R}^d \rightarrow \mathbb{R}$ :

$$\psi(z, \mathbf{p}) = \psi_{\text{ch}}(z) + \psi_{\text{int}}(\mathbf{p}), \quad \psi_{\text{ch}}(z) = \alpha_1 z + \frac{1}{2} \alpha_2 z^2 + z \log(z) + (1 - z) \log(1 - z), \quad \psi_{\text{int}}(\mathbf{p}) = \frac{1}{2} \kappa |\mathbf{p}|^2, \quad (1)$$

with the material parameters  $\alpha_1, \alpha_2 \in \mathbb{R}$  and  $\kappa > 0$ . The resulting dimensionless Cahn–Hilliard-type phase field model seeks the normalized lithium concentration  $c: [0, T] \times \bar{\Omega} \rightarrow [0, 1]$  and the chemical potential  $\mu: [0, T] \times \bar{\Omega} \rightarrow \mathbb{R}$  satisfying

$$\begin{cases} \partial_t c = \nabla \cdot (m(c) \nabla \mu) & \text{in } (0, T) \times \Omega, \\ \mu = \partial_z \psi(c, \nabla c) - \nabla \cdot \partial_{\mathbf{p}} \psi(c, \nabla c) & \text{in } (0, T) \times \Omega, \end{cases} \quad (2)$$

with the nonlinear isotropic mobility  $m(z) = Dz(1 - z)$ ,  $D > 0$ . As boundary conditions we neglect surface wetting, meaning  $\nabla c \cdot \mathbf{n} = 0$ , and assume a given particle surface flux  $N_{\text{ext}} < 0$  modeling the lithium insertion by  $-m(c) \nabla \mu \cdot \mathbf{n} = N_{\text{ext}}$ . At initial time we prescribe a constant concentration profile  $c(0, \cdot) = c_0 \in (0, 1)$ .

## 3 Parallel Matrix-Free Finite Element Solver

According to [2, 3], we discretize the model equations (2) in space with fourth-order Lagrangian finite elements and perform the time integration with the NDF( $k$ ) family of linear multistep methods,  $k \in \{1, \dots, 5\}$ , in a variable-step, variable-order algorithm [6]. Advancing one time step requires solving a nonlinear problem using Newton's method. To solve the linear

\* Corresponding author: e-mail fabian.castelli@kit.edu, phone +49 721 608 48736, fax +49 721 608 43490



This is an open access article under the terms of the Creative Commons Attribution-NonCommercial License, which permits use, distribution and reproduction in any medium, provided the original work is properly cited and is not used for commercial purposes.

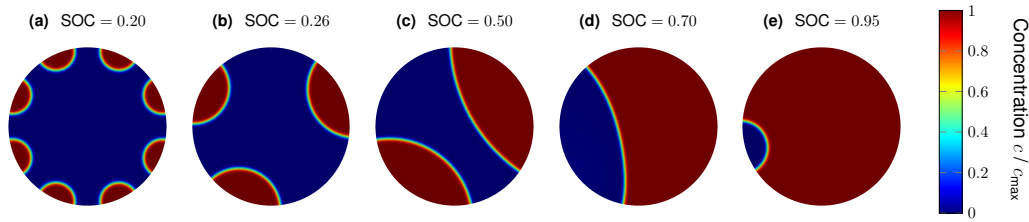


**Fig. 1:** Concentration profile for  $N_{\text{ext}} = 1 C$  at various SOC.

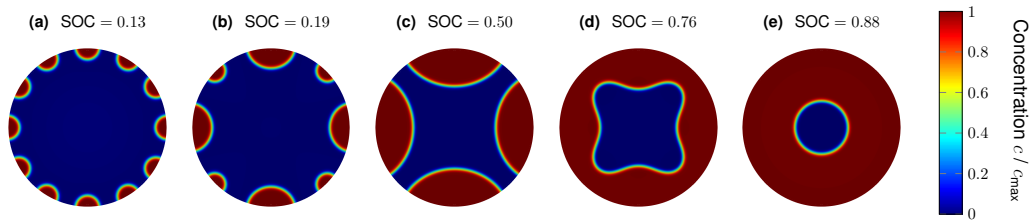


**Fig. 2:** Concentration profile for  $N_{\text{ext}} = 10 C$  at various SOC.

systems with the GMRES method in each Newton step we have proposed a specialized preconditioner in [2, 3], which incorporates the nonlinear mobility and, in particular, allows the parallel matrix-free implementation with the functionalities of the finite element library *deal.II* [7].

#### 4 Insertion-Rate Dependent Phase Morphologies

We simulate the lithiation of a two-dimensional circular LFP particle choosing the material parameters from [2, Sect. 6.2.2] with two different insertion rates  $N_{\text{ext}} \in \{1 C, 10 C\}$ .

In Figs. 1 and 2 we visualize the concentration profile at various state of charges (SOC). Note the relation  $\text{SOC}(t) = c_0 + t$  between time and state of charge in our case. We observe different phase morphologies for the two insertion rates. Starting from a symmetric concentration profile, an intercalation wave develops in Fig. 1. On the other hand, in Fig. 2 we see a core-shell scenario forming. This dependence of the phase morphology on the insertion rate is in qualitative accordance to the recently developed scaling law in [8], even though we neglected the mechanical coupling here.

Both simulations are performed on a node of parallel computer with 96 GB RAM and 20 Intel Xeon Silver 4114 CPUs with 2.2 GHz. In particular, matrix-free computations used the 256 bit AVX register. The computational time depends heavily on the developing phase morphology. For  $N_{\text{ext}} = 1 C$ , the coarsening process, the generation and traveling of the intercalation wave needs approx. 2000 time steps and the computation takes approx. 18 hours. The formation of the core-shell scenario requires approx. 1000 time steps and is calculated in approx. four hours. In both cases our matrix-free preconditioner is robust and allows us to avoid storing matrices, thus saving the assembly time and a large amount of memory. In average, we need approx. 80 (for  $N_{\text{ext}} = 1 C$ ) and approx. 50 (for  $N_{\text{ext}} = 10 C$ ) GMRES iteration steps without restart.

**Acknowledgements** G.F.C. acknowledges financial support by the German Research Foundation (DFG) through the Research Training Group 2218 SiMET – Simulation of mechano-electro-thermal processes in lithium-ion batteries, project number 281041241. Open access funding enabled and organized by Projekt DEAL.

#### References

- [1] G. F. Castelli, L. von Kolzenberg, B. Horstmann, A. Latz, and W. Dörfler, *Energy Technol.* **9**(6), 2000835 (2021).
- [2] G. F. Castelli, Numerical Investigation of Cahn–Hilliard-Type Phase-Field Models for Battery Active Particles, PhD thesis, Karlsruhe Institute of Technology (KIT), 2021, To be published.
- [3] G. F. Castelli and W. Dörfler, Study on an adaptive finite element solver for the Cahn–Hilliard equation, in: *Numerical Mathematics and Advanced Applications ENUMATH 2019*, edited by F. J. Vermolen and C. Vuik, *Lect. Notes Comput. Sci. Eng.* Vol. 139 (Springer, Cham, 2021), pp. 245–253.
- [4] T. Zhang and M. Kamlah, *Electrochim. Acta* **298**, 31–42 (2019).
- [5] L. Wu, V. D. Andrade, X. Xiao, and J. Zhang, *ASME J. Electrochem. En. Conv. Stor.* **16**(4), 041006 (2019).
- [6] L. F. Shampine and M. W. Reichelt, *SIAM J. Sci. Comput.* **18**(1), 1–22 (1997).
- [7] W. Bangerth, R. Hartmann, and G. Kanschat, *ACM Trans. Math. Software* **33**(4), Art. 24, 27 (2007).
- [8] D. Fraggedakis, N. Nadkarni, T. Gao, T. Zhou, Y. Zhang, Y. Han, R. M. Stephens, Y. Shao-Horn, and M. Z. Bazant, *Energy Environ. Sci.* **13**(7), 2142–2152 (2020).